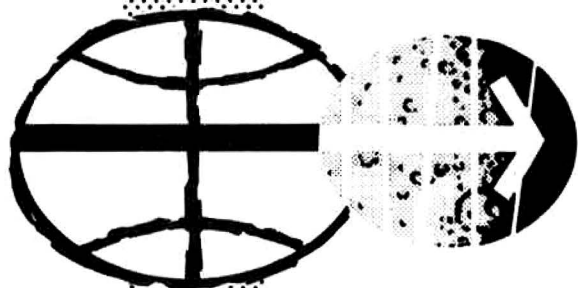




NATIONAL AERONAUTICS AND SPACE ADMINISTRATION

APOLLO 13 MISSION
HIGH-GAIN ANTENNA ACQUISITION PROBLEM

ANOMALY REPORT 2



MANNED SPACECRAFT CENTER
HOUSTON, TEXAS
December 1970

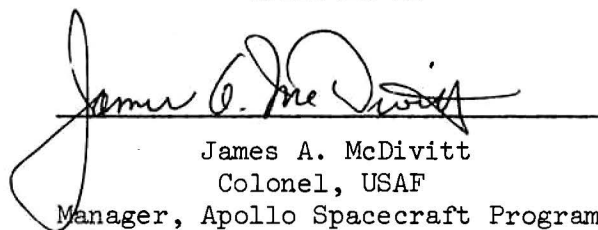
APOLLO 13 MISSION
HIGH-GAIN ANTENNA ACQUISITION PROBLEM

Anomaly Report 2

PREPARED BY

Mission Evaluation Team

APPROVED BY



James A. McDivitt
Colonel, USAF
Manager, Apollo Spacecraft Program

NATIONAL AERONAUTICS AND SPACE ADMINISTRATION
MANNED SPACECRAFT CENTER
HOUSTON, TEXAS
December 1970

STATEMENT

Prior to the television transmission at approximately 55 hours, difficulty was experienced in obtaining high-gain antenna acquisition and subsequent tracking.

At 55:00:10, the reacquisition mode was selected. Starting at 55:00:10 and continuing to 55:00:40, deep repetitive transients were noted approximately every 5 seconds on the phase-modulated downlink carrier and the antenna would not lock up and track.

DISCUSSION

At the time of the anomaly, the antenna boresight axis was approximately 35° away from the line-of-sight to the ground station because, 7 hours earlier, the Command Module Pilot had manually adjusted the antenna to the ground-requested settings of plus 23° in pitch and 267° in yaw. The most favorable settings for 55 hours were actually plus 5° in pitch and 237° in yaw. When the transmission was switched from the omnidirectional antenna to the manual mode of the high-gain antenna, there was a 6-dB decrease in uplink signal strength and a 17-dB decrease in downlink signal strength. With the high-gain antenna in the wide-beam mode and nearly boresighted, the uplink and downlink signal strengths should have been at least equal to the signal strength obtained with the omnidirectional antenna. A comparison of the wide-, medium-, and narrow-beam transmit and receive patterns indicates that the high-gain antenna was in the medium-beam, manual mode at the time of acquisition and remained in this configuration until the reacquisition mode was selected at 55:00:10. Starting at 55:00:10 and continuing to 55:00:40, deep repetitive transients occurring approximately every 5 seconds were noted on the phase-modulated downlink carrier (fig. 1).

System testing with a similar antenna and electronics box showed RF signatures comparable to those observed in flight. These signatures were obtained by placing the target inside the scan limit and the manual setting outside the scan limit. These two positions were separated approximately 35° , matching the flight angular separation. Under these conditions, the antenna cycled between the scan limit and the manual setting while operating in the automatic-reacquisition mode and produced the cyclic RF signature. Since the inflight line-of-sight to earth was not near the scan limit, the failure mechanism would be a shift in the scan-limit and scan-limit-warning function lines, as illustrated in figure 2. These function lines would have to shift such that they would both be positioned between the antenna manual setting and the true line-of-sight to earth. Also, the antenna would have to be operating in the auto-reacquisition mode to provide these signatures.

The antenna functions which caused the cyclic inflight RF signatures resulting from a shift in the function lines can be explained with the aid of figures 1 and 2, with the letters A, B, C, and D corresponding to events during the cycle. Starting at approximately 55:00:10, the antenna was switched from manual to auto reacquisition with the beam select switch in the medium-beam position. From point A to the scan-limit function line just prior to point B, the antenna acquired the earth in wide beam. When the antenna reached the scan-limit function line, the antenna control logic switched the system to the manual mode and drove back toward the manual settings until the scan-limit-warning function line at point C was reached, thereby maintaining wide-beam operation. When the antenna reached the scan-limit-warning function line, the system automatically switched to the medium-beam mode and continued to drive in the manual mode until the manual setting error was nulled out at point A. The antenna control logic then switched to the auto-track mode and repeated the cycle. The most important feature of this cycle is that the antenna moved at the manual scan rate between points B and D, which is confirmed by the rapid changes in the downlink signal strength.

The scan-limit and scan-limit-warning functions are generated by the C- and A-axis angles. The C- and A-axes are shown in figure 3. Figure 4 shows the scan-limit and scan-limit-warning function lines in the antenna coordinate (C- and A-axes) system. The C-axis and A-axis angle signals are generated in the high-gain antenna gimbals by two separate induction transducers. The C-axis signal comes from a linear induction potentiometer. The A-axis signal comes from a device similar to a synchro resolver. The A-axis signal is then half-wave, phase-sensitive demodulated, and the C-axis signal is half-wave rectified. The two signals and a dc bias are then summed by a differential amplifier shown on figure 5. The output of this summing amplifier is then compared to another dc bias voltage in a second differential amplifier. When the output of the first amplifier exceeds the dc bias supplied to the second amplifier, the second amplifier switches, indicating to the antenna logic that the scan-limit line has been reached. A similar circuit implements the scan-limit-warning line.

System analysis and tests rejected the following possible causes for the problem:

a. The high-gain antenna is pointed using 3 gimbals (fig. 3). The B-axis is nulled out for A-axis and C-axis tracking and is used only for tracking where the boresight to the target passes close to the end of the antenna boom. The B-axis drive is then used to eliminate the requirement for high A-axis slewing rates. B-axis offset could not have caused the problem because if a maximum possible offset of about 20° existed, the A-axis and C-axis track loops would have detected and nulled out the offset without driving into the scan limit.

b. A failure of any single component in the RF system including feed lines, strip lines, switching diodes, and hybrids would produce a beam misalignment (servo null misalignment) between wide and narrow beams. For beam misalignments less than 3° , the antenna would lock up in narrow beam, which is normal. For beam misalignments greater than 3° , the antenna would oscillate between wide and narrow beam but would remain in automatic track. Neither of the above two conditions would cause the antenna to switch between automatic track and manual mode and this is required to cause the high slewing rates that are necessary to explain the characteristics of the downlink signal strength transients.

c. Elements in the scan-limit and scan-limit-warning circuits were shorted and opened to determine the effect on the scan-limit functions. The results of this test shifted the scan-limit functions, but did not produce the necessary change in the scan-limit slope. Consequently, a failure in the electronic box is ruled out.

The only component identified with a failure mode that would produce a shift in the scan-limit functions and a slope change is the C-axis induction potentiometer located in the antenna. This potentiometer (fig. 6) is used to provide a voltage proportional to the C-axis angular orientation. It consists of three separate coils, each with a symmetrical winding on opposite sides of the rotor or stator. These coils include the primary winding on the stator: the compensation, or bias, winding on the stator; and the linear output winding located on the rotor. The bias winding is used to shift the normal $\pm 70^\circ$ linear output to a new linear output over the range of from minus 10° to plus 130° .

Shorting one-half of the primary winding of the stator to ground would produce a greater slope in the curve of the induction potentiometer output voltage compared with angular travel. This short would also produce nonlinear effects because the magnetic flux would be concentrated in one-half of the primary winding. The normal transfer function of the potentiometer and the transfer function required to produce the flight anomaly are shown in figure 7.

The electrical, mechanical, and thermal stresses applied to the C-axis induction potentiometer during manufacture were investigated and found to be well within the design capability of the potentiometer. Manufacturing processes used were also examined but no deficiencies were found. In addition, no similar failure has previously occurred. Since review of the potentiometer design and the processes used in its manufacture revealed no inadequacies, no corrective action can be taken to prevent recurrence of the problem.

The induction potentiometer scale factor and linearity are last checked during gimbal assembly acceptance testing at the antenna supplier's plant. Consequently, the potentiometer could have been shorted when the antenna was delivered to the launch site.

CONCLUSIONS

Most probably, a short occurred in the primary winding of the C-axis induction potentiometer which resulted in an effective shift in the scan-limit and scan-limit-warning functions.

CORRECTIVE ACTION

Tests have been added at the launch site to ensure proper scan-limit and scan-limit-warning functions prior to flight. In addition, a procedure has been developed to determine acceptable spacecraft attitudes for high-gain antenna operation in the event another scan-limit shift occurs on a future flight.

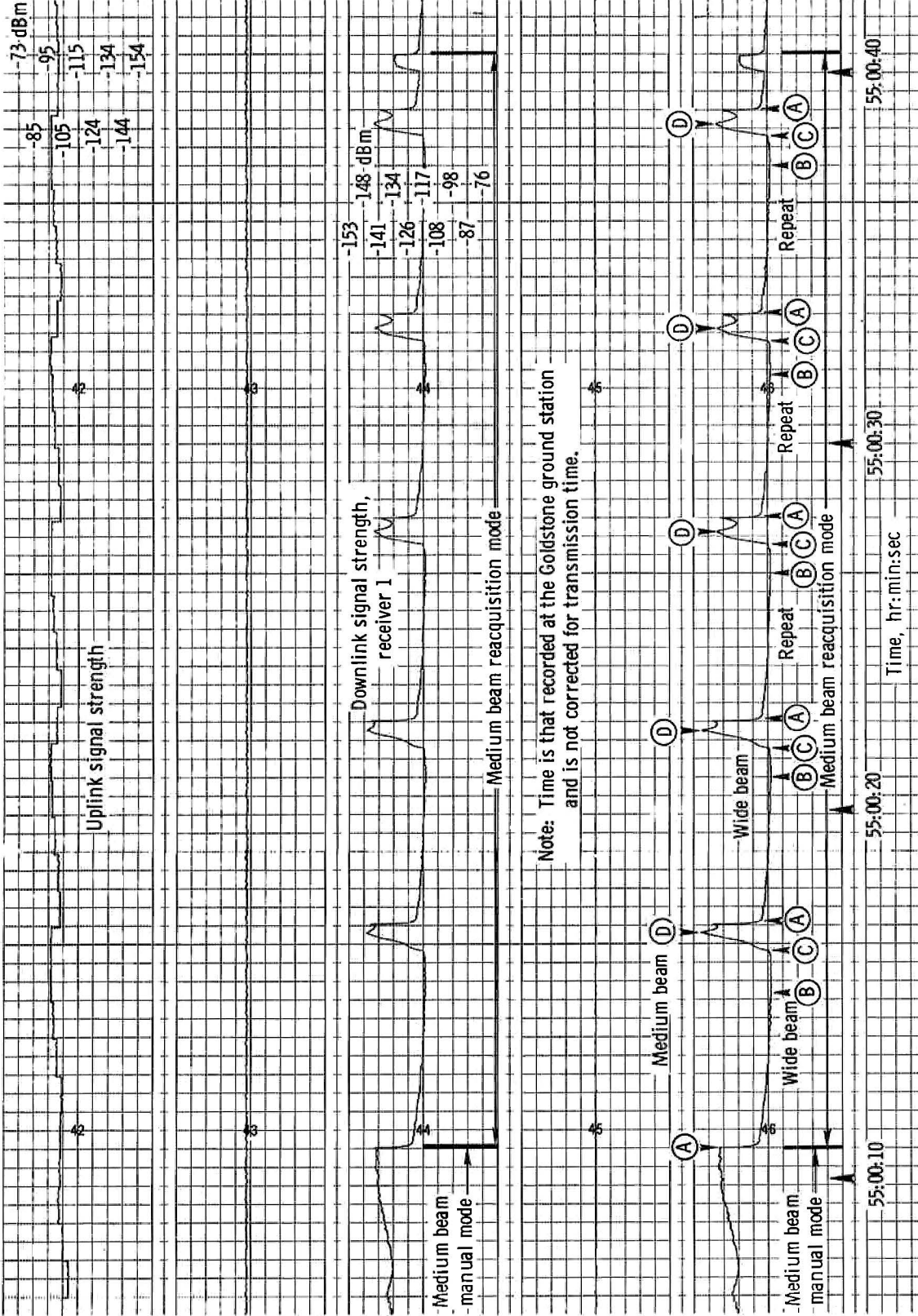


Figure 1. - Recorded signal strengths during high gain antenna operation.

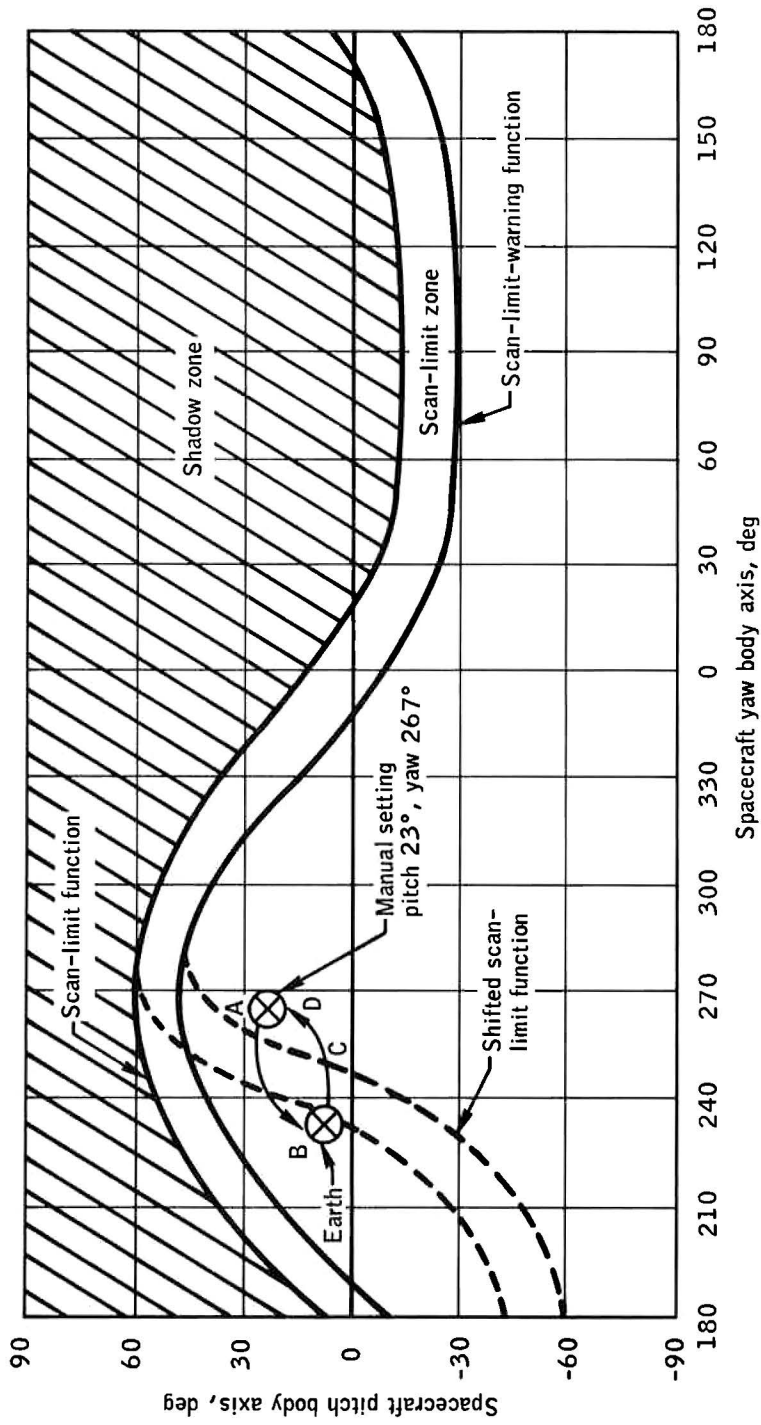


Figure 2.- Shift in scan-limit and scan-limit-warning function lines.

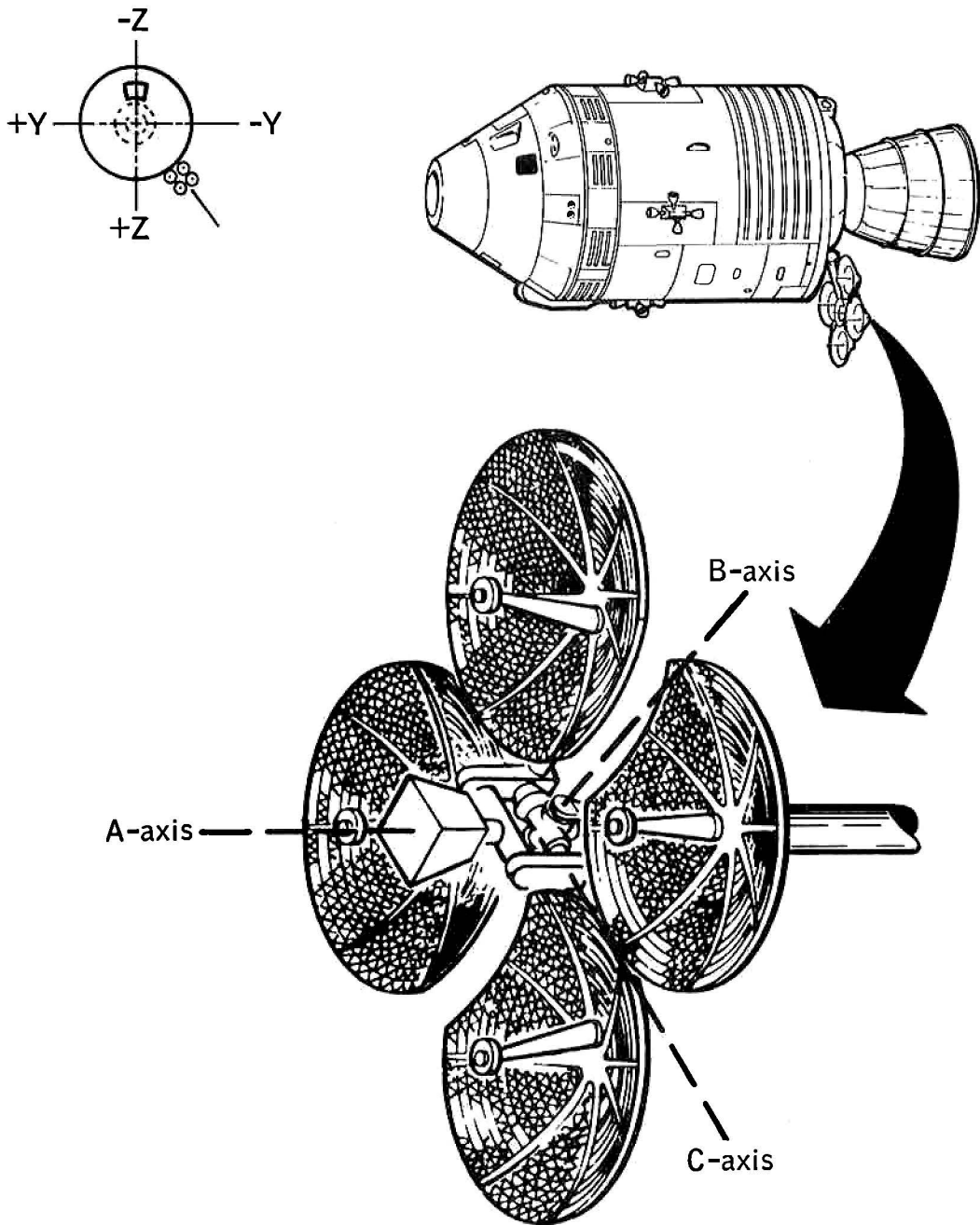


Figure 3.- Antenna gimbal axes.

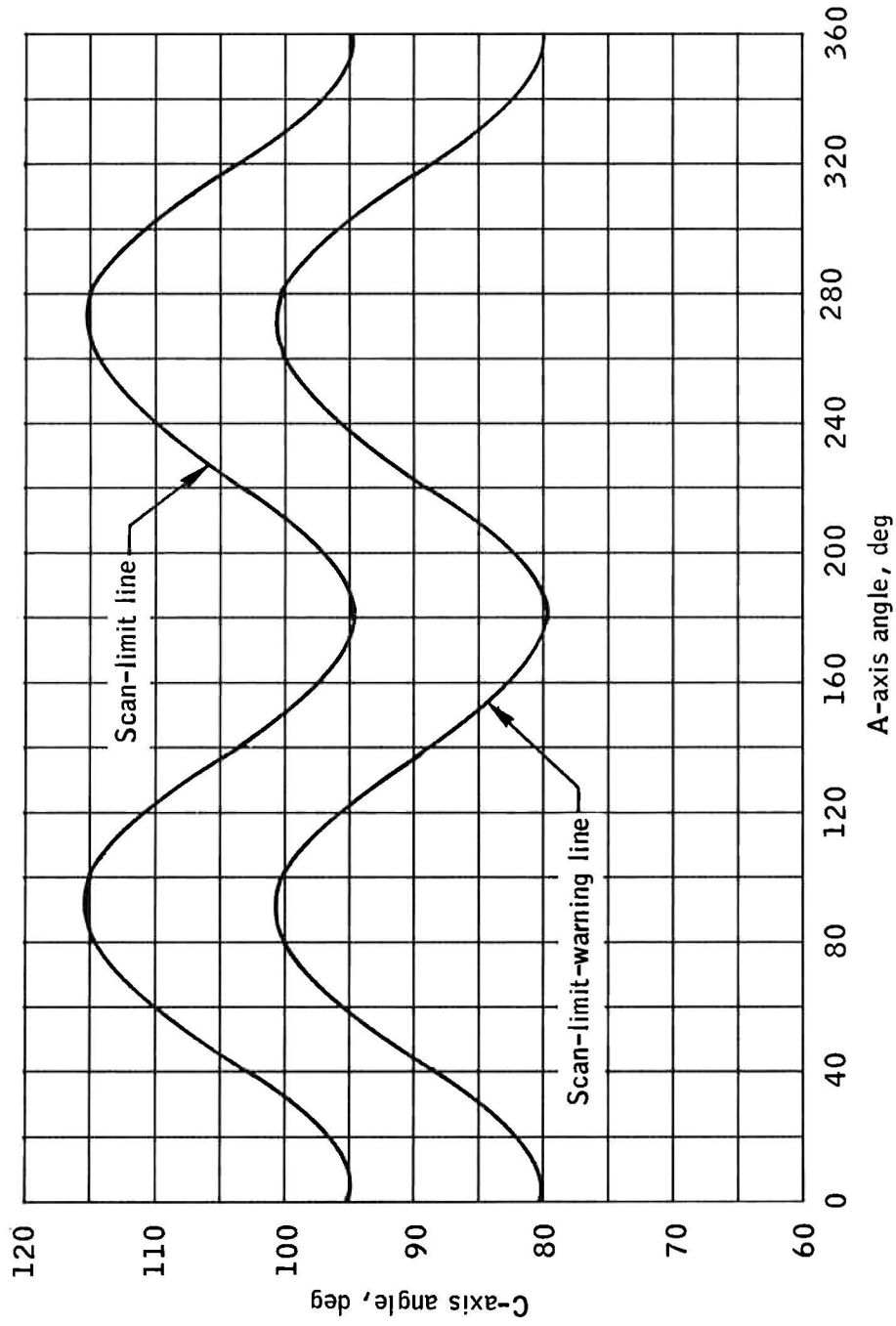


Figure 4.- Scan-limit and scan-limit-warning lines in antenna coordinates.

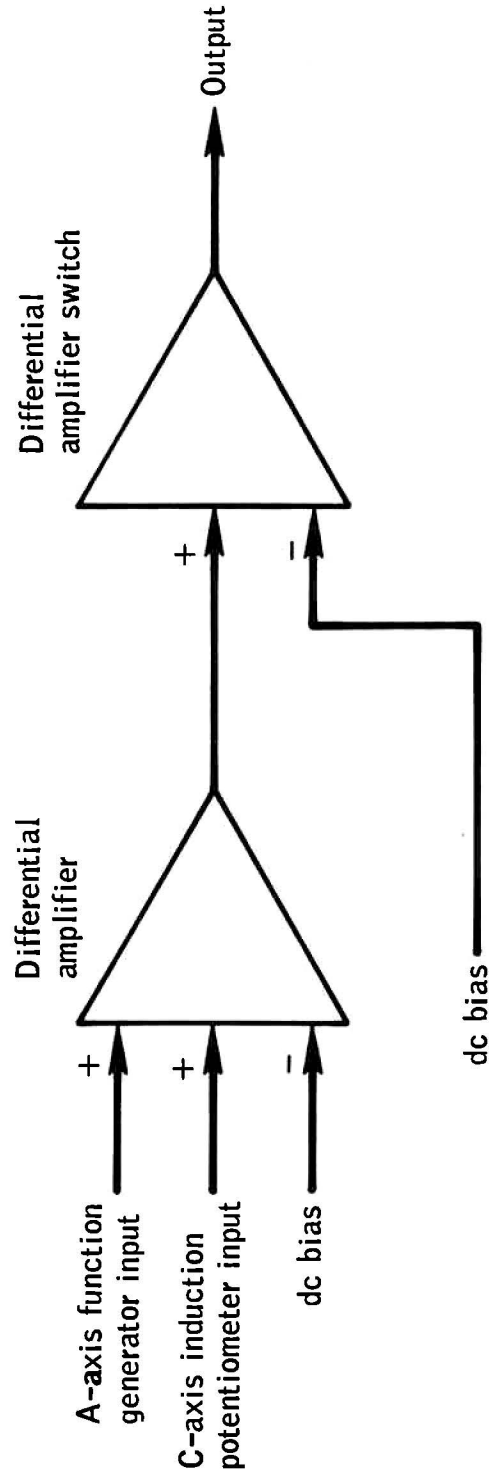


Figure 5.- Limit logic circuit .

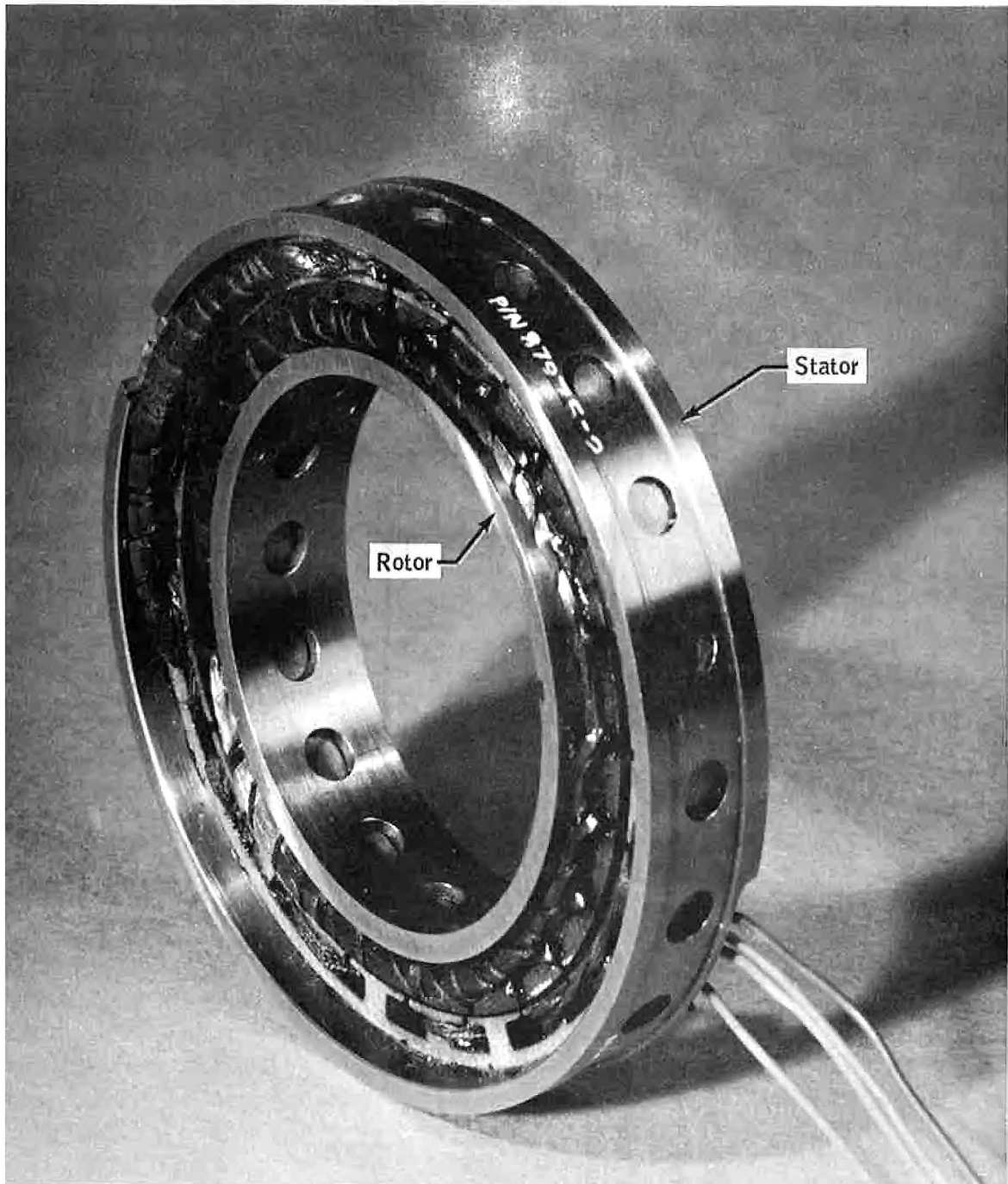
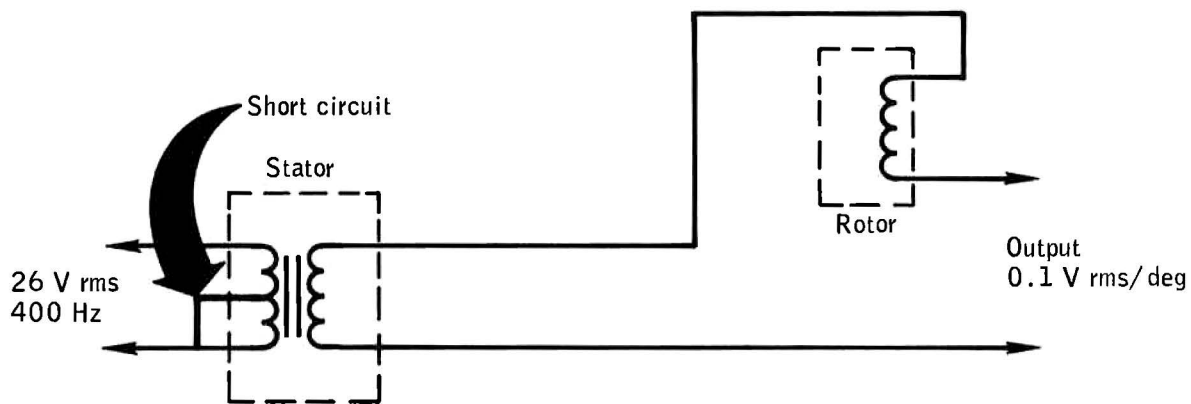
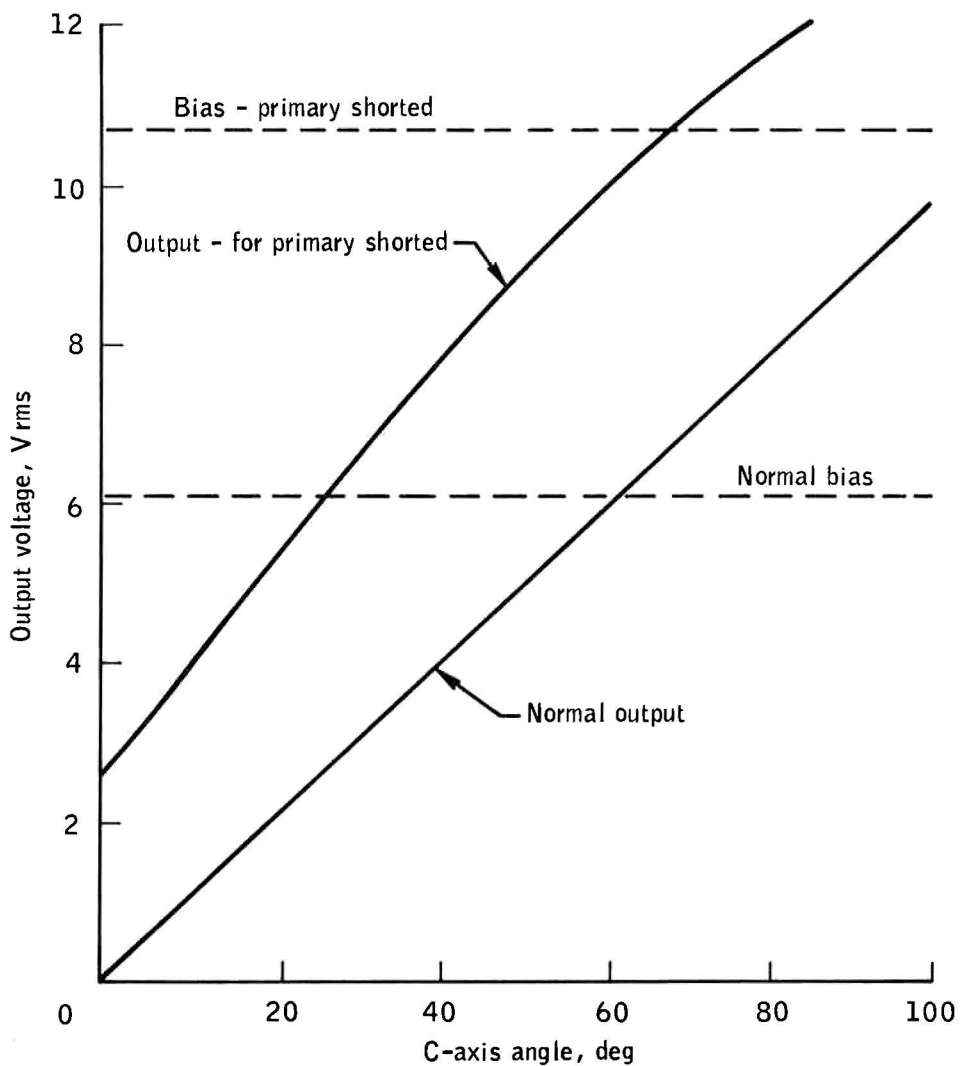


Figure 6.- C-axis induction potentiometer.



(a) C-axis induction potentiometer schematic.



(b) C-axis induction potentiometer voltages for normal and shorted primary.

Figure 7.- C-axis induction potentiometer schematic and operational characteristics.

